THE BEHAVIOR OF ANODIZED Zr AT HIGHER TEMPERATURE IN ORAL CAVITY

Maria VARDAKI[1], Sabina-Magda POPA[2], Stefania-Alina BUZINCU[3], Ioana DEMETRESCU[4,5]

Abstract. *The aim of the present paper is investigation of behavior at different temperature in oral cavity of anodized Zr in two different conditions. The anodizing procedure was performed in two different mixtures of NH_4F and distilled water in glycerol leading to two electrolytes (E1, E2) of the same substances, but with different concentrations. Regarding the other anodizing conditions, the anodizing voltage and time were the same for both electrolytes being 3 different voltages (20 V, 40 V and 60 V) and 1 hour. Anodized samples characterization included surface analysis and electrochemical stability in Afnor saliva at different temperature, taking into account that in oral cavity the temperatures could be different. Surface analysis as scanning electronic microscopy (SEM) was completed with contact angle determinations and electrochemical procedures have been represented by potentiodynamic polarization curves (Tafel curves) and electrochemical impedance spectroscopy. As conclusion surface analysis demonstrated the different lengths and diameters of nanotubes ZrO_2 obtained after anodizing at different voltage and higher hydrophilic character with the voltage elaboration increase. Regarding the electrochemical stability, for samples fabricated in both electrolytes were observed higher corrosion rates at higher temperatures and smaller activation energy.*

Keywords: ZrO_2 nanotubes, SEM, electrochemical tests, Afnor saliva, activation energy

1.Introduction

Generally speaking biomaterials materials are chosen as a function of their biocompatibility, mechanical properties, electrochemical stability and price [1-3]. The development of material for dental use has the same motivations in selection, but is more dynamic in promoting materials materials taking into account the esthetic factor as well. Zirconium, nowadays an alternative for Ti the golden reference in dental applications, is a valve metal and as Ti [4] has a natural passivation ceramic oxide formed spontaneously on the surface. Zr has a higher density than Ti (6.52g/cm^3) but a convenient Young's modulus as 88 GPa and a lateral shear strength of 33 GPa. Zr native passive film on the surface named "zirconia" with the formula ZrO_2, has osseointegration better when compared to titanium [5] and in the oral cavity, is not affected by plaque accumulation. This

[1]PhD, Depart. of General Chemistry, University Politehnica of Bucharest, Romania, (e-mail: vardaki_m@hotmail.com).
[2]Master, Depart. of General Chemistry, University Politehnica of Bucharest, Romania (sabinapopa54@gmail.com).
[3]Master, Depart. of General Chemistry, University Politehnica of Bucharest, Romania, (e-mail buzincu.stef@gmail.com).
[4]Prof, Depart. of General Chemistry, University Politehnica of Bucharest, Romania (ioana_demetrescu@yahoo.com).
[5] Academy of Romanian Scientists, 54 Spaiul Independentei, 050094, Bucharest, Romania

oxide is representative for advanced ceramic group with various important applications having high strength, fracture toughness, chemical and thermal stability, and biocompatibility [6,7] Regarding the processing procedures of metallic biomaterials, anodizing was found as the cheapest, and very flexible method of nano architectures formation, having the possibility to obtain various dimensions by changing anodizing conditions [8-10]. Nanotube fabrication by anodizing on valve metals such as Zr and Ti is controlled by electrolyte composition, pH, temperature and applied voltage as the most important parameters [11-13]. At the first stage of anodizing, zirconium is forming a barrier-type layer under applied field which grows predominantly by the inward migration of anions [9]. The pore formation leads to nanotubular structure formation as the expression of result of processes of electric field assisted dissolution and chemical dissolution of the barrier layer. Zirconia nanotubes was fabricated as well in two steps anodizing [14]. Depending of anodizing parameters some nanostructures om Zr alloys remain nanopores and other lead to nanotubes structure [15].

The present paper aim is elaboration of ZrO2 nanotubes via anodizing in two electrolytes differing in concentration of glycerol and their characterization. The fabricated nanostructures have various morphology being elaborated at three different voltage such as 20,40and 60 V respectively. As a result, their hydrophilicity and electrochemical stability are different. Their corrosion rates determined at different temperatures permitted discussion about significant corrosion rate increase at higher temperature [16] and evaluation of activation energy. It is to mention that the present study is useful for patients due to the fact that despite the fact that in the oral cavity the metallic materials used for restorative works are supposed to be exploited at different temperatures, usually there are investigations only at human body temperature.

2. Materials and methods

2.1. Samples preparation and anodizing procedure

Zr foils of 99.98% purity and 0.1 mm thickness (Sigma-Aldrich) were ground with SiC paper 1200, washed in an ultrasound bath with acetone, ethanol and distilled water for 5 minutes each and finally dried in atmosphere at room temperature. Nanostructures were obtained on the Zr surface *via* anodizing technique performed in a typical two electrodes electrochemical cell, where the Zr samples were used as working electrode and a Pt electrode as counter electrode. Two different mixtures of NH_4F and distilled water in glycerol were prepared for the anodizing, leading to two electrolytes (E1, E2) of the same substances, but with different concentrations. In Table 1 are presented the concentrations of NH_4F and distilled water, used for the preparation of the glycerol-based electrolytes. As

E1 is noted the first solution used for the anodizing of the samples, while as E2 the second one.

Table 1. Substances concentrations of the glycerol-based electrolytes

Substance	Concentration (%)	
	E1	**E2**
NH_4F	0.74	0.5
Distilled water	15	5
Glycerol	84.26	94.5

The anodizing took place at 3 different voltages (20 V, 40 V and 60 V) for an hour. After the anodizing the samples were immersed for 20 minutes in ethanol, then rinsed thoroughly with distilled water and finally dried in atmosphere at ambient temperature. Finally, the samples were annealed in air for an hour at 450 ◦C.

2.2. Surface analysis

The surface morphologies of the Zr samples were investigated with a Quanta 650 scanning electron microscope (SEM) from FEI in high vacuum at 10 kV. The length and the diameters of the formed nanostructures were established from the obtained micrographs.

The hydrophilic/hydrophobic balance was evaluated from contact angle measurements using a CAM 100 equipment. All the measurements were performed with distilled water. The contact angle values represent the average of 5 measurements.

2.3. Electrochemical stability

The electrochemical behavior of the samples was investigated by a Potentiostat/Galvanostat Autolab PGSTT 402 equipped with the software of Nova 1.10. As test solution was used the Afnor artificial saliva, whose composition is presented at the next table [17].

Table 2. Afnor artificial saliva recipe

Substance	**NaCl**	**KCl**	**Na_2HPO_4**	**$NaHCO_3$**	**KSCN**	**CH_4ON_2 (Urea)**
Concentration (g/L)	0.7	1.2	0.26	1.5	0.33	1.3

Electrochemical procedures have been represented by potentiodynamic polarization curves (Tafel curves) and electrochemical impedance spectroscopy

((the applied amplitude of the alternating current potential was 10 mV and impedance spectra were acquired in the frequency range of 10^{-1} Hz and 10^4 Hz). For the electrolyte E1 the electrochemical measurements were performed, also, at three different temperatures in order to calculate the activation energies. The activation energy can be calculated using the Arrhenius graphs and Eq. (1):

$$i_{corr} = Ae^{-Ea/RT} \quad (1)$$

where A is a constant called preexponential factor, Ea is the activation energy of the process expressed in J/mol, R is the universal gas constant (8.314 J/ (mol K)) and T is the temperature in K.

3. Results and discussion

3.1. Surface analysis

3.1.1. SEM results

Fig. 1 shows the surface of Zr samples anodized in E1 or E2 at 20 V. As can be seen from the Fig. 1a the surface of the sample anodized at E1 at 20V is formed of porous oxide. The pores have no uniform size and shape, while the smallest diameters are approximately around 20 nm. Based on the Fig. 1b, the anodization at 20 V resulted in the formation of narrow and long nanotubes with a diameter of 10-20 nm and lengths of 1.5-2 μm. Above the nanotube layer there is a thick layer of compact oxide about 2 μm thick. It is to mention that the morphology presented in Fig. 1, 2, 3 is in total accord with literature data [18-20] regarding nanotubes ZrO2 formation in mixture with organic electrolyte in comparison with nanotubes formation in first generation of anodizing for nanotubes synthesis. In the frame of anodizing [21] with inorganic fluoride mixture, the diameter increases approximately linearly with an increasing anodizing voltage, but tubes wall thickness remain approximately constant The diameter increases approximately linearly with an increasing anodization voltage, but tubes wall thickness stays almost constant As expected longer tubes can be obtained using organic electrolytes based on more glycerol and at the same voltage the glycerol addition slightly disturbs the order of obtained oxide nanostructure and strongly slows down the oxide layer growth rate. At 40 V, anodizing in E1led to a surface composed of a layer of porous oxide and a layer of nanotubes exposed where the porous layer has dissolved shown in Fig. 2a. The diameters of the nanotubes are about 30 nm and the diameters of the nanopores are about 15 nm. The electrolyte E2 produced at 40 V led to an increased size of the nanotubes to approximately 20 nm in diameter and 2 μm in length (Fig. 2b). The compact oxide layer is thinner, porous and absent in some places.

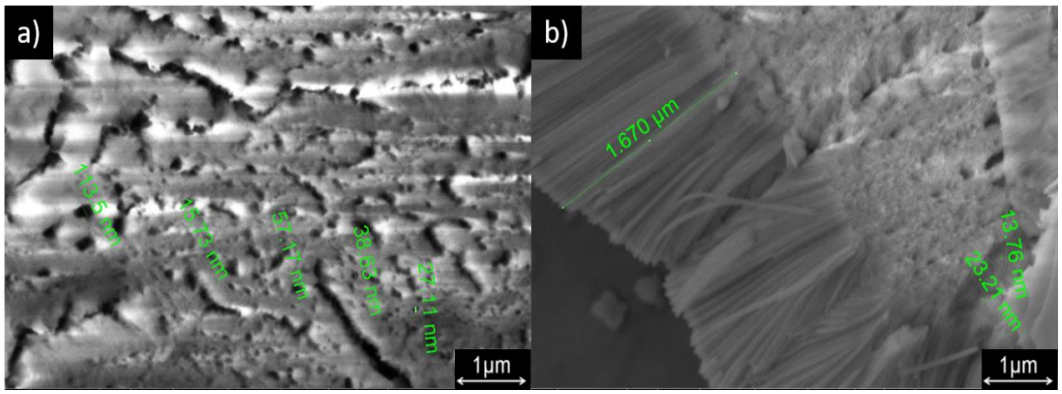

Fig. 1. SEM micrographies for Zr samples anodized at 20 V in a) E1, b) E2

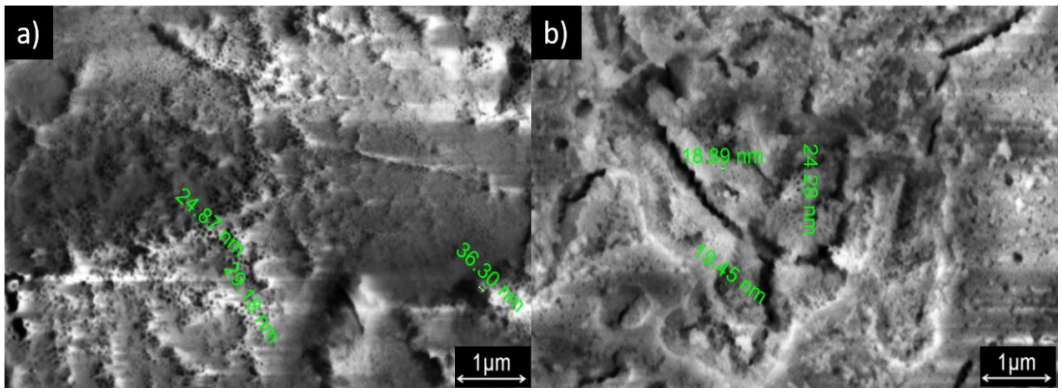

Fig. 2. SEM micrographies for Zr samples anodized at 40 V in a) E1, b) E2

The surface of the anodized sample at 60 V in the E2 consists of a layer of nanotubes with diameters between 20 and 40 nm and residual porous oxide remaining undissolved (Fig. 3a). For the sample anodized in the electrolyte E2 the increase of the applied voltage to 60 V resulted in the complete dissolution of the compact oxide layer and the nanotubes being discovered (Fig. 3b). The diameters of the nanotubes vary between about 20-30 nm and the lengths are over 2 µm.

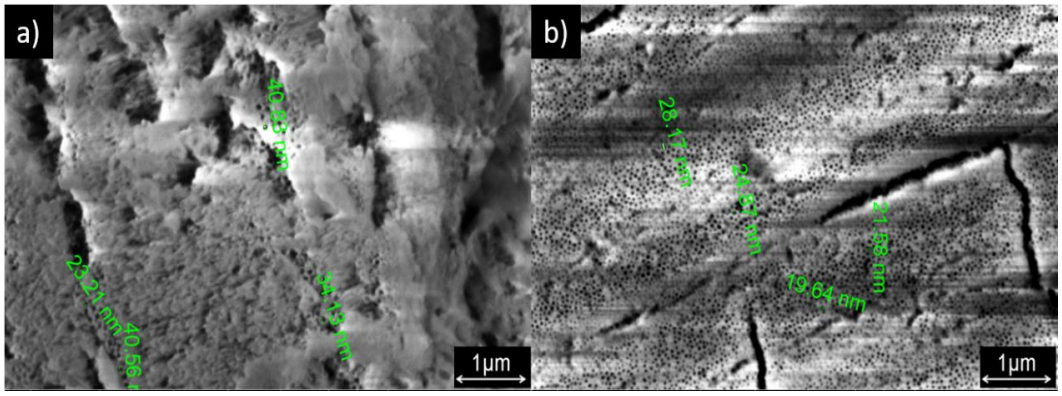

Fig. 3 SEM micrographies for Zr samples anodized at 60 V in a) E1, b) E2

3.1.2. Contact angle measurements

Table 3 presents the results of the contact angle measurements for the Zr anodized samples. As it can be seen, the electrolyte used for the anodizing affected the obtained contact angle values. The values for the samples anodized in E1 are smaller than the samples anodized in E2, indicating that the E1 electrolyte led to more hydrophilic surfaces.

Table 3. Contact angle measurements

Applied voltage (V)	**Contact Angle (◦)**			
	Anodized		**Air annealed**	
	E1	**E2**	**E1**	**E2**
(Non-anodized Zr)	73.40		44.49	
20	19.20	60.45	18.22	32.76
40	14.91	26.08	13.93	23.01
60	12.81	18.37	9.53	13.86

Moreover, it can be observed that after the air annealing treatment the values of the samples, for both electrolytes, was a bit decreased. All the samples no matter in what electrolyte were anodized, obtained contact angle values in the hydrophilic domain even in the super hydrophilic (value less than 10◦). Accordingly, the increase of the applied voltage leads to a more hydrophilic character of the sample. Nevertheless, all the samples anodized at a voltage bigger than 20 V present a higher hydrophilic character in comparison with the non-anodized sample (0 V), which presents the lowest hydrophilicity from all the samples.

3.2. Electrochemical analysis

3.2.1. Tafel polarization curves

Figure 4 shows the potentiondynamic curves of the Zr samples anodized in E1 or E2. Based on the figures of the Tafel polarization curves, it can be said that the Zr anodized at 20 V is the one that offers the highest resistance to corrosion, since its corrosion rate is smaller than the other samples.

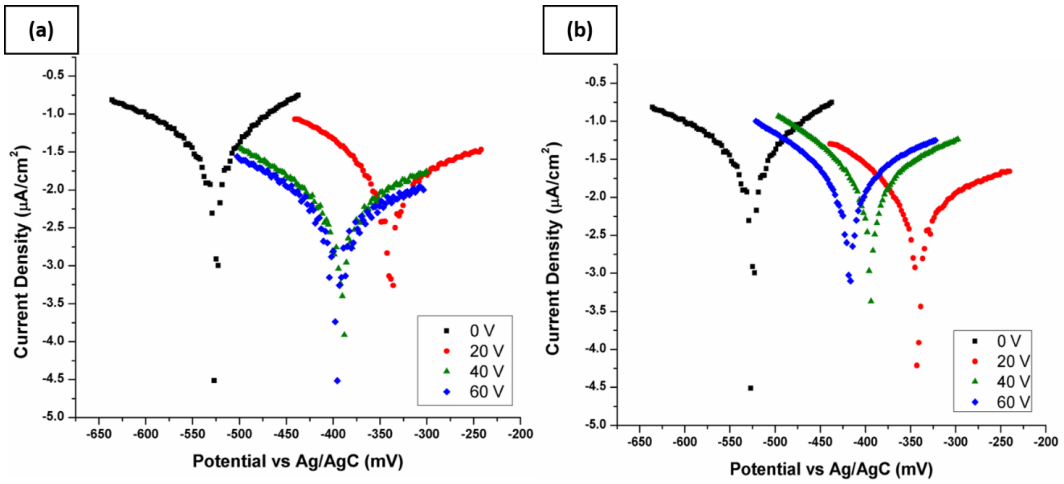

Fig. 4 Tafel polarization curves of samples anodized in: (a) E1, (b) E2

Moreover, the sample that wasn't anodized seems to present a higher corrosion rate and thus its resistance to corrosion is lower than the rest of the samples. Consequently, the anodizing technique seems to enhance the samples' resistance to corrosion (Table 4).

Table 4. Corrosion parameters of samples anodized in E1or E2

Anodizing electrolyte	Applied voltage (v)	i_{corr} (nA·cm^{-2})	E_{corr} (mV)	V_{corr} (µm·year^{-1})	R_p (MOhm·cm)	B_a (mV)	B_c (mV)
	0	113.63	-525.97	6.67	0.7122	42.42	47.96
	20	8.71	-340.63	0.10	5.909	97.82	375.24
	40	15.54	-391.60	0.18	4.459	183.43	190.90
	60	17.64	-397.86	0.20	1.909	113.29	255.69
	20	30.09	-233.16	1.30	1.5890	117.69	165.18
	40	32.97	-417.14	1.52	1.5370	215.65	254.69
	60	60.60	-392.58	2.78	1.3857	251.60	835.51

Based on the data of the above table, it can be said that the Zr sample anodized at 20 V is the one that presents the most increased stability based on its

corrosion parameters for both used electrolytes. The samples anodized at 20 V are having the lowest corrosion rate and density.

The corrosion density of the anodized samples presents some differences. These variations are, probably, due to flaws or non-uniformities of the developed nanostructures.

It was also noticed that the sample that wasn't anodized (0 V), has a higher current density (icorr) than the rest of the samples which they were, no matter what was the applied voltage or the electrolyte. Moreover, the lower the value of current density, the more protective and more stable can be considered the sample.

3.2.2. Activation energy

The activation energy of an electrochemical process refers to the energy level that is required for an electron to have in order to pass through the interface of the electrode-electrolyte. Hence, when the activation energy is low, a high corrosion rate is observed. Moreover, based on the Arrhenius equation a high activation energy indicates as well a high temperature dependence of the corrosion rate. In Fig. 5 are presented the polarization curves of Zr samples anodized in E1 and then tested electrochemically at three different temperatures. The polarization method was performed in Afnor saliva.

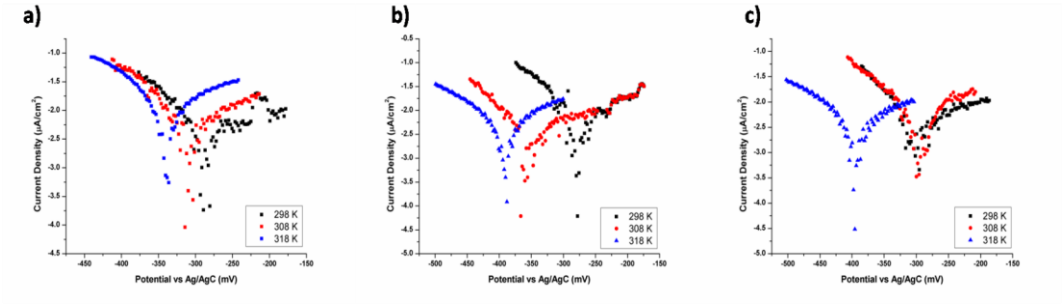

Fig. 5. Tafel polarization curves of samples anodized in E1 at a) 20V, b) 40 V, c) 60 V

According to Fig. 5, it seems that the increase of the temperature of the Afnor artificial saliva affected the corrosion resistance of the samples. Being more precisely, as the temperature of the saliva increases, the corrosion rate increases as well and, hence, the resistance to corrosion gets weaker.

From Table 5 it can be observed that the increase of the temperature resulted in the enhancement of the corrosion, lowering the stability of the samples. Nonetheless, the sample anodized at 20 V and tested in Afnor saliva, which was heated up to 298 K is the one presenting the lowest corrosion rate from all the others samples anodized in different voltages and tested in different temperatures.

Table 5. Corrosion parameters for E1 anodized samples in Afnor artificial saliva at different temperatures

Applied voltage (v)	Temperature (k)	i_{corr} ($nA \cdot cm^{-2}$)	E_{corr} (mV)	V_{corr} ($\mu m \cdot year^{-1}$)	R_p (MOhm·cm)	B_a (mV)	B_c (mV)
	298	8.71	-340.63	0.10	5.909	97.82	375.24
	308	22.84	-286.21	0.15	3.722	70.53	110.25
	318	32.41	-306.23	0.16	3.138	129.70	290.62
	298	15.54	-391.60	0.18	4.459	183.43	190.90
	308	19.35	-296.24	0.19	2.588	123.35	139.14
	318	21.56	-342.08	0.25	1.890	114.37	216.07
	298	17.64	-397.86	0.20	1.909	113.29	255.69
	308	19.37	-282.45	0.21	3.051	127.34	344.32
	318	23.76	-287.02	0.23	1.581	96.14	284.48

The activation energy was calculated from the Arrhenius plots and the Eq. (1), while in Table 6 are shown the parameters which were calculated from Eq. (1).

Table 6. Activation energy of Zr samples

Applied Voltage (V)	Ea (j/mol)	A
20	54623	25.13
40	13593	0.00000348
60	12388	0.00000236

As can be seen from Table 6 the activation energy for corrosion in saliva for samples fabricated at higher voltage is much smaller indicated a more rapid process.

3.2.3. EIS measurements

EIS measurements were also performed in order to clearly understand Zr samples' behavior in the used artificial saliva (Afnor saliva). From the figures below, it can be noticed a linear slop in Bode plots of log |Z|, while in Bode plots of phase-angle is demonstrating practically a capacitive nature of the samples over a broad area of frequencies as the maximum value of phase angle is around 80°. Furthermore, the Bode plots, as it can be seen, are "divided" in two different areas, one located at frequencies of the high range and the other one at frequencies of low range. The electrolyte's resistance is the cause of the frequencies of the high range, while the capacitance of the surface's film is responsible for the frequencies of low range (Figs. 6-8).

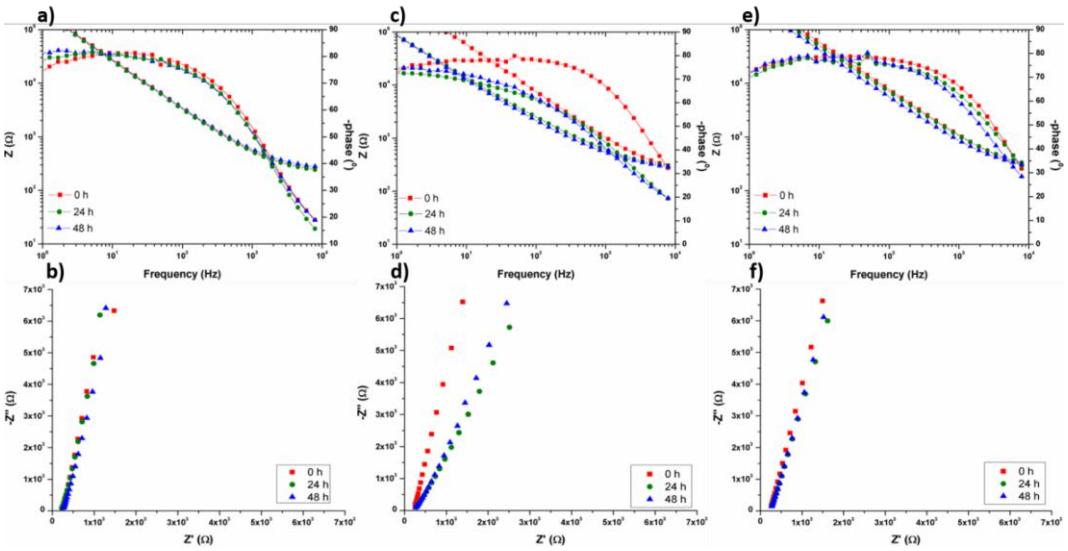

Fig. 6. Bode and Nyquist plots for samples anodized in E1 at (a,b) 20 V, (c,d) 40 V, (e,f) 60 V

The Nyquist plots are presented in Figs. (6-8) and based on them it can be noticed that the curves of the capacitive loops are dependent to the immersion time in the Afnor testing saliva. More precisely, the increase of the immersion time results to a small increase of the curve, implying that a protective film that was formed on the samples' surface was getting thicker and, thus, offers a better protection against the corrosion.

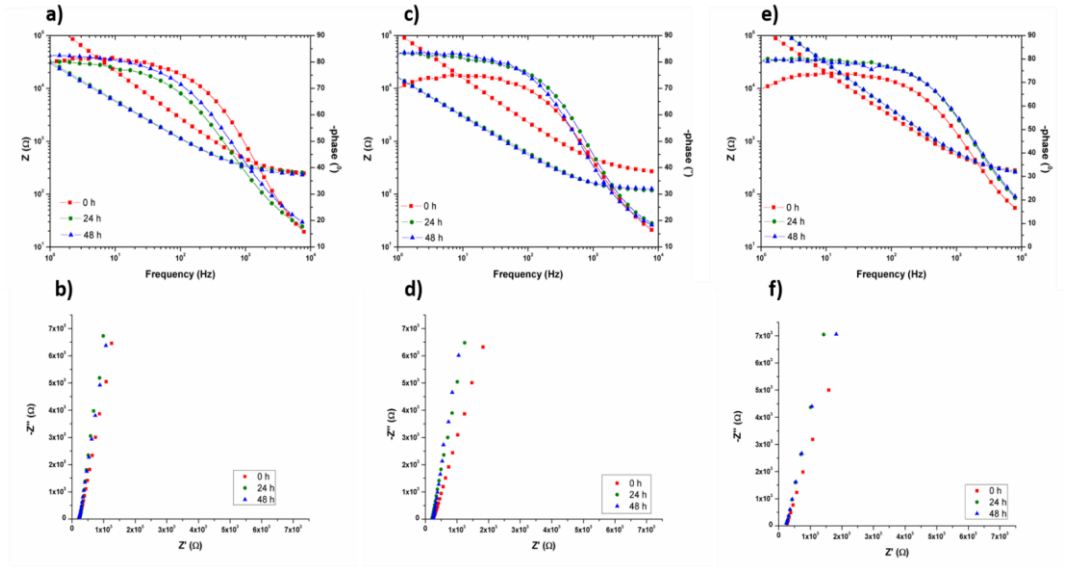

Fig. 7. Bode and Nyquist plots for samples anodized in E2at (a,b) 20 V, (c,d) 40 V, (e,f) 60 V

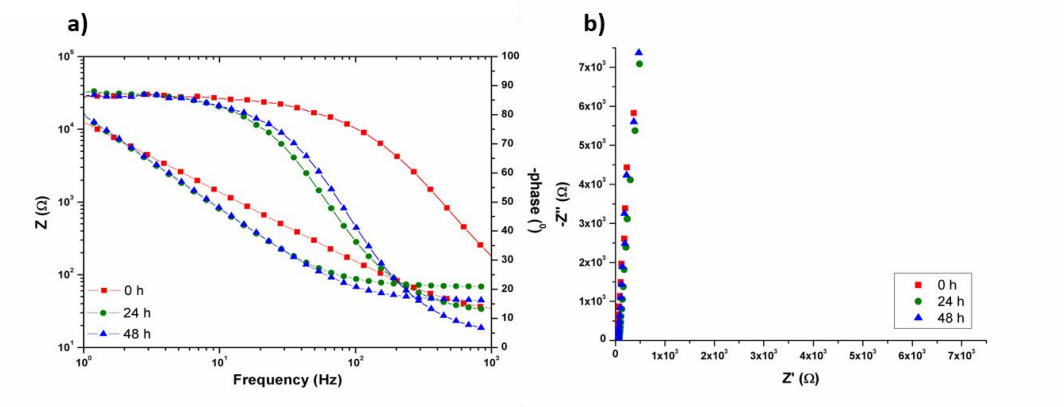

Fig. 8. Bode (a) and Nyquist (b) plots for non-anodized Zr sample

The equivalent circuits were developed by the process of data fitting of the recording EIS spectra. The circuits are presented in Figs. 9-11 Moreover, Table 7 shows the EIS parameters obtained after fitting the equivalent circuits.

The R1 stands for the electrolyte's resistance, while the substrate's polarization resistance as well as the coating's (the obtained nanostructure) resistance, are expressed as R3 and R2, respectively. Moreover, the CPE1 symbolizes the double layer capacitance expressed at the interface electrolyte-nanostructure and the CPE2 is due to the heterogenity of the film. When the parameter n is close to 0 that means that the sample presents a resistance behavior, while when the n is close to 1 that means that the sample has a capacitance behavior. Here, the samples present a n close to 0.9 meaning that they are stable. Moreover, it can be observed that after of 24 h of immersion in the saliva the samples started to show a more capacitive behavior. Figures 9-11 present the equivalent circuits of the samples in E1 or E2 and in different applied voltages.

Table 7. Electrochemical parameters for fitted EIS circuits anodized in E1 or E2

Anodizing electrolyte	Applied voltage (V)	Time (h)	R1 (KΩ·cm^2)	R2 (KΩ·cm^2)	R3 (KΩ·cm^2)	CPE 1	CPE2	C1 (μF·cm^{-2})	C2 (μF·cm^{-2})
						n1	**n2**		
-	0 (Non-anodized)	0	23	7.10	-	0.639	0.962	-	-
		24	64.1	15.1	-	0.845	0.963	-	-
		48	39.0	13.7	-	0.446	0.963	-	-
E1	20	0	2.39	729	832	0.901	-	4.56	-
		24	2.15	314	768	0.914	-	1.26	-
		48	2.53	121	691	0.819	-	1.28	4.93
	40	0	1.16	295	218	0.886	-	-	-
		24	2.27	133	523	0.753	-	3.32	11.9
		48	2.23	662	101	0.738	-	3.31	7.47
	60	0	2.30	183	281	0.794	0.944	-	-
		24	2.25	58.9	193	0.698	0.929	-	-
		48	2.62	109	289	0.877	0.953	1.13	-
E2	20	0	241	3.73	-	0.905	-	870	-
		24	127	12.7	486	0.936	-	357	1.97
		48	201	15.6	201	0.917	-	514	2.17
	40	0	256	3.97	530	0.842	0.951	-	-
		24	205	4.81	513	0.770	-	578	1.78
		48	218	2.07	167	0.919	-	900	4.66
	60	0	253	4.11	506	0.837	0.946	-	-
		24	229	5.79	218	0.785	-	883	-
		48	220	4.80	150	0.772	-	867	-

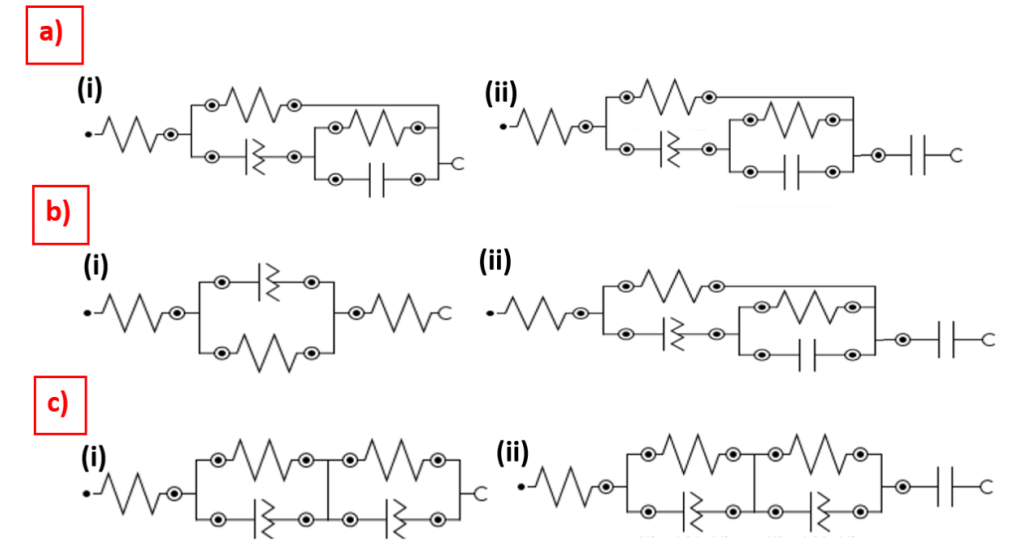

Fig. 9 EIS fitted circuits for samples anodized in E1 at: a) 20 V after: (i) 0 h and 24 h, (ii) 48 h in afnor saliva, b) 40 V after: (i) 0 h, (ii) 24 h and 48 h in afnor saliva, c) 60 V after: (i) 0 h and 24 h, (ii) 48 h in afnor saliva

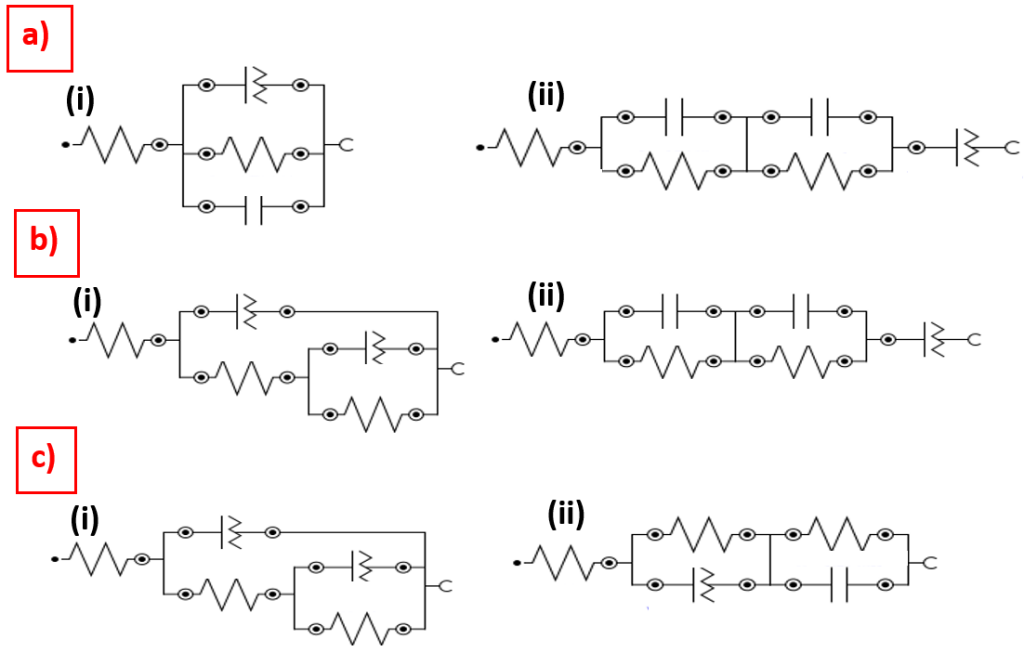

Fig. 10 EIS fitted circuits for samples anodized in E2 at: a) 20 V after: (i) 0 h, (ii) 24 h and 48 h in afnor saliva, b) 40 V after: (i) 0 h, (ii) 24 h and 48 h in afnor saliva, c) 60 V after: (i) 0 h, (ii) 24h and 48 h in afnor saliva

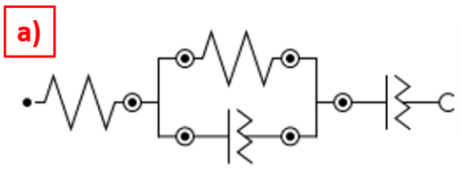

Fig. 11 EIS fitted circuits for non-anodized Zr sample after: a) 0 h, 24 h and 48 h in afnor saliva

Conclusions

In this paper we studied aspects of the behavior of anodized Zr at higher temperature in oral cavity. After anodizing at three voltage in two mixtures with different concentrations of glycerol, the same surface analysis and electrochemical stability tests at various temperatures in Afnor saliva were performed. The scanning electronic microscopy (SEM) indicated different lengths and diameters of nanotubes ZrO_2 obtained after anodizing and contact angles measurements evidenced higher hydrophilic character with the voltage elaboration increase. Regarding the electrochemical stability, for samples elaborated in both electrolytes were observed higher corrosion rates at higher temperatures and smaller activation energy.

Acknowledgments

This work was supported by CNCSIS–UEFISCSU, project number PN-III-P4-ID PCE 2016-0316.

R E F E R E N C E S

1. Niinomi M., (2008), Metallic biomaterials, *J. Artif. Organs*, **11 (3)**, 105-110.

2. Popa M.V., Demetrescu I., Vasilescu E., Drob P., Ionita D., (2005), Stability of some dental implant materials in oral biofluids, *Rev. Roum. Chim.*, **50 (5)**, 399-406.

3. Popa M.V., Vasilescu E., Drob P., Demetrescu I., Popescu B., Ionescu D., (2003), In vitro assessment and monitoring of the implant titanium materials–physiological environment interactions, *Mater. Corros.* **54 (4)**, 215-221.

4. Demetrescu I., (2008), Passive and bioactive films on implant materials and their efficiency in regenerative medicine, *Mol Cryst Liq Cryst.*, **486(1)**,110/ [1152]-119/ [1161].

5. Bernhard N., Berner S., De Wild M., Wieland M., (2009), The binary TiZr Alloy - a newly developed Ti alloy for the use in dental implants, *Forum Implantol.*, **5**, 30-39.

6. Gomez Sanchez A., Schreiner W., Duffó G., Ceré S., (2011), Surface characterization of anodized zirconium for biomedical applications, *Appl Surf Sci*, **257 (15)**, 6397-6405.

7. Gomez Sanchez A., Katunar M., Schreiner W., Duffó G., Ceré S., Schiffrin D.J., (2014), Structure and dielectric properties of electrochemically grown ZrO2 films, *Acta Chim. Slov.* **61**, 316–327.

8. Guo L., Zhao J., Wang X., Xu X., (2009) Structure and bioactivity of zirconia nanotube arrays fabricated by anodization, *Int. J. Appl. Ceram. Technol*., **6**, 636–641.

9. Yasud, K., Schmuki, P., (2007), Formation of self-organized zirconium titanate nanotube layers *Adv. Mater.*, **19**, 1757–1760.

10. Stoian A.B., Demetrescu I., Mazare A., Dinischiotu A., Nica C., Ionita D., (2018), Electrochemical stability and cell response of nanostructures elaborated on zirconium, *Mat Corros*, **69 (8)**, 1039-1046.

11. Tsuchiya H., Schmuki P., (2004), Thick self-organized porous zirconium oxide formed in H2SO4/ NH4F electrolytes, *Electrochem. Commun*., **6 (11)**, 1131–1134.

12. Guo L., Zhao J., Wang X., Xu R., Lu Z., Li Y., (2009), Bioactivity of zirconia nanotube arrays fabricated by electrochemical anodization, *Mater. Sci. Eng.: C*, **29**, 1174–1177.

13. Ismail S., Ahmad Z., Berenov A., Lockman Z., (2011), Effect of applied voltage and fluoride ion content on the formation of zirconia nanotube arrays by anodic oxidation of zirconium, *Corros. Sci.*, **53**, 1156–1164.

14. Chen Y., Zhang G., Shen Z., (2015), Two-step anodization fabrication of ordered ZrO2 nanotube arrays, *J Aus Cer Soc.*, **51(2),** 29-35.

15. Stoian A.B., Vardaki M., Ionita D., Enachescu M., Prodana M., Brancoveanu O., Demetrescu I., (2018), Nanopores and nanotubes ceramic oxides elaborated on titanium alloy with zirconium by changing anodization potentials, *Cer Intern.*, **44 (6),** 7026-7033.

16. Nie X.H., Li X.G., Du C.W., Cheng Y.F., (2009), Temperature dependence of the electrochemical corrosion characteristics of carbon steel in a salty soil, *J. Appl. Electrochem.*, **39 (2)**, 277–282.

17. Romonti D.E., Gomez Sanchez A.V., Milošev I., Demetrescu I., Ceré S., (2016), Effect of anodization on the surface characteristics and electrochemical behaviour of Zr in artificial saliva, *Mater Sci. and Eng. C,* **62**, 458-466.

18. Stępień M., Handzlik P., Fitzner K., (2014), Synthesis of ZrO_2 nanotubes in inorganic and organic electrolytes by anodic oxidation of zirconium, *J Solid State Electr*, **18 (11)**, 3081–3090.

19. Schmuki P., Berger S., (2008), Enhanced self-ordering of anodic ZrO2 nanotubes in inorganic and organic electrolytes using two-step anodization, *Phys Status Solidi (RRL)*, **2 (3)**, 102–104.

20. Minagar S., Berndt C.C., Wang J., Ivanowa E., Wen C., (2012), A review of the application of anodization for the fabrication on nanotubes on metal implant surfaces, *Acta Biomater*., **8 (8)**, 2875–2888.

21. Ismail S., Ahmad Z.A., Berenov A., Lockman Z., (2011), Effect of applied voltage and fluoride ion content on the formation of zirconia nanotube arrays by anodic oxidation of zirconium, *Corros Sci* **53 (4)**, 1156–1164.